Energy Reports 7 (2021) 4951–4960

Contents lists available at ScienceDirect

Energy Reports

journal homepage: www.elsevier.com/locate/egyr

Research paper

Optimal design and analysis of DC–DC converter with maximum power controller for stand-alone PV system

Djaafar Toumi [b], Djiliani Benattous [b], Ahmed Ibrahim [a,*], H.I. Abdul-Ghaffar [c], Sergey Obukhov [d], Raef Aboelsaud [a], Yacine Labbi [b], Ahmed A. Zaki Diab [e]

[a] Electrical Power & Machines Department, Faculty of Engineering, Zagazig University, Egypt
[b] VTRS-Research Laboratory, University of El-Qued, B.P. 789, 39000 El-Qued, Algeria
[c] Mechatronics Department, Egyptian–Korean Faculty for Industry and Energy Technology, Bani Swief Technological University, Bani Swief, Egypt
[d] National Research Tomsk Polytechnic University, Tomsk 634050, Russia
[e] Electrical Engineering Department, Faculty of Engineering, Minia University, Minia 61111, Egypt

ARTICLE INFO

Article history:
Received 6 May 2021
Accepted 19 July 2021
Available online xxxx

Keywords:
Photovoltaic stations
Maximum power controller
DC–DC buck converter
Matlab/Simulink
sampling time

ABSTRACT

This paper proposes a method for selecting the parameters of the main components of an autonomous photovoltaic (PV) stations to ensure the most efficient conversion and use of solar energy. The main energy characteristics are analyzed and the mathematical models of the components of an autonomous PV system are developed to study the modes of tracking the maximum power point (MPP). The necessary conditions for matching the parameters of the PV and the DC–DC buck converter are evaluated to track the MPP. This paper aims to create an original method and algorithm for calculating and selecting parameters of the main elements of a PV stations. The optimal value of the sampling time of the MPP controller is obtained for different schemes of the PV system . A practical example is considered for selecting the parameters of a DC–DC buck converter and a digital MPP of an autonomous PV station. The simulation of dynamic modes of an autonomous photovoltaic (PV) station is performed in the MATLAB/SIMULINK software package. The simulation results of dynamic operations of the PV system show that the voltage converter and the MPP controller with the selected parameters according to the proposed method provide reliable and effective tracking of the MPP in all different connections of the PV.

1. Introduction

One of the most promising technologies for the production of electric energy is the photovoltaics (PV), which over the last few years has shown the greatest development in comparison with other types of renewable energy sources. The installed capacity of PV stations in 2017 reached 408 GW and attracted 58% of all new investments in renewable energy or $ 161 billion (Jäger-Waldau, 2018). The environmental friendliness and widespread availability of solar energy determine good prospects for the use of PV systems in Russia, especially in the microgeneration sector, and significant measures for this are taken by government support measures (Anon, 0000; Ashurov et al., 2019; Renewable energy policy network for the 21st century (REN21), 2018). In recent years, about 240 MW of photovoltaic generating capacities have been installed in Russia, and the total installed capacity of photovoltaic power plants (taking into account the Crimean Solar Power Station in 2018) exceeded 600 MW (Avezova et al., 2019).

The main problems in the practical application of PV are the relatively low efficiency of primary energy conversion and the pronounced dependence of the energy characteristics of solar cells on external climatic conditions. In order to increase energy efficiency, most modern PV systems are built using the technology of maximum power point tracking (MPPT), which allows to increase electricity generation from 30 to 40%. This technology is based on three main interconnected components: the MPPT method, the MPPT controller and the DC–DC power converter. The non-linearity of the current–voltage characteristics of the solar panel and their dependence on illumination and temperature make the design of the main components of the PV system highly difficult. For autonomous PV system, the solution to this problem is complicated by the fact that they can significantly vary in topology, types of DC–DC converters and the uses of MPPT controllers. Moreover, the well-known methods for selecting the parameters of DC–DC converters with the subsequent synthesis of control systems (Chetti, 1990; Mack, 2008), which are widely

* Corresponding author.
E-mail addresses: ibragim@tpu.ru (A. Ibrahim), abdelghafar_ibrahim@yahoo.com (H.I. Abdul-Ghaffar), a.diab@mu.edu.eg (A.A.Z. Diab).

https://doi.org/10.1016/j.egyr.2021.07.040

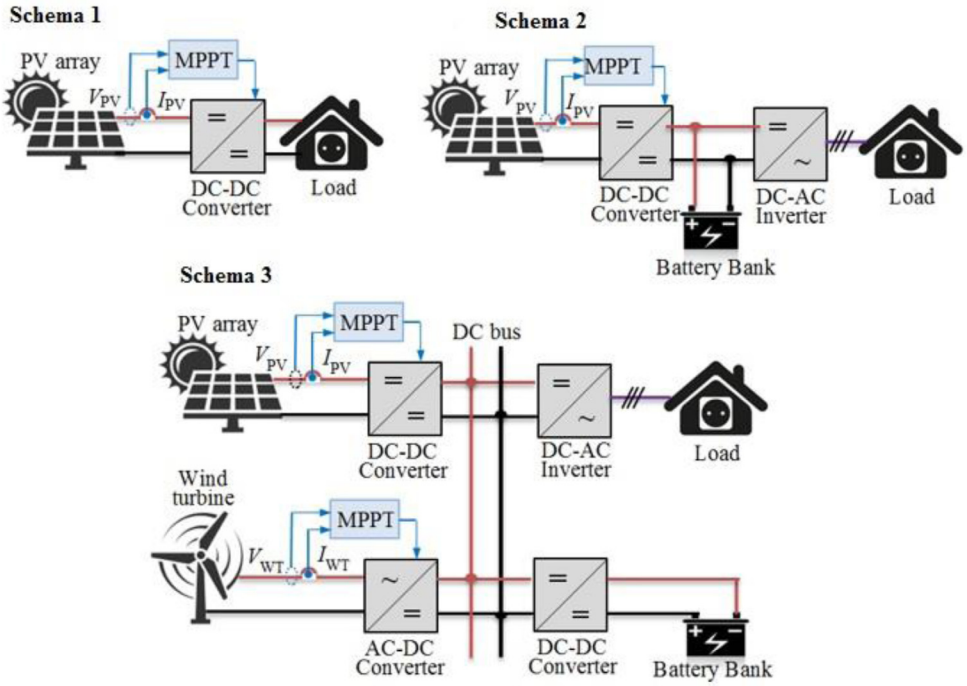

Fig. 1. A typical block diagram of the construction of Autonomous photovoltaic stations.

used in the design of traditional power sources, are unacceptable for solving this problem.

The purpose of the research was to develop a methodology for selecting the parameters of the main components of an autonomous PV, providing the most efficient conversion of solar energy. To test and verify the results obtained, simulation modeling of the dynamic regimes of the PV was used in the MATLAB/Simulink® software package.

The remainder of this paper is organized in the following manner. Section 2 describes the objective of the research and the statement of the problem. Section 3 elaborates on basic technical characteristics and mathematical models of autonomous PV components. Section 4 deals with the conditions for matching the parameters of a solar panel and a voltage converter for MPPT. Section 5 discusses the choice of optimal parameters of the main elements of PV system. The simulation results considering the validation of the proposed algorithm under uniform solar irradiance and fast changes of the solar insolation are presented in Section 6. In the conclusion section, the research findings are recapitulated.

2. Object of research and problem statement

The system of research of this work is the PV system which is designed to provide the electric power to the consumers in isolation from the central electrical network. From the point of view of the basic architecture, three main options can be distinguished for constructing autonomous PV (Fig. 1).

In the simplest configuration (Schema 1), the PV includes only the PV array and a DC–DC converter operating under the control of the MPPT point search controller. The advantages of this type of PV are maximum simplicity and low cost, an obvious disadvantage is the low reliability of power supply to consumers. The area of the practical application of such stations is heating, cooking and pumping water systems that are not critical to the supply voltage parameters (Nayak et al., 2017). The main function of the control system of such a PV is to maximize the use of available solar energy without the need to control the output voltage and current of the DC–DC converter.

Autonomous PV systems with energy storage devices, which mainly use rechargeable batteries (Battery Bank), are more widely used. The use of battery bank can significantly increase the reliability of the PV and provide consumers with the electricity of the required quality, but the cost of the PV and the complexity of the control system increase. Depending on the purpose, in practice, two main options are used to build autonomous PV power plants with energy storage: energy systems with a single generating source (Schema 2) and hybrid energy complexes, in addition to photomultiplier stations, other plants are also used as generation sources, for example, wind energy (Schema 3).

Note that there are other ways to build autonomous PV and hybrid energy systems (Khatib et al., 2016; Chauhan and Saini, 2014). The choice for analysis of the three presented in Fig. 1, the topologies are explained by the fact that they differ from each other in the nature of the electric load of the DC–DC converter, which has a direct effect on its dynamic characteristics, and, accordingly, on the selection of parameters of all the main elements of the PV. For all other PV topologies not considered in this paper, the operation modes of the DC–DC converter will be similar to one of the above cases.

It should also be noted that various types of voltage converters are used as part of autonomous PV, a detailed review and comparative analysis of which are presented in Amir et al. (2019) and Obukhov et al. (2016a). In these studies, autonomous PV based on a buck DC–DC converter, which is mainly used in low-power energy systems, is considered as an object of analysis. Also, in this paper, we do not consider modes of partial shading of PV panels, which are especially critical for high-power photovoltaics, requiring the use of specialized MPPT controllers (Obukhov et al., 2016a; Rezk et al., 2017).

The research objectives were to analyze the static and dynamic characteristics of the DC–DC converter and MPPT controller of an autonomous PV, as well as to develop, on the basis of the results obtained, a practical methodology for choosing their optimal parameters.

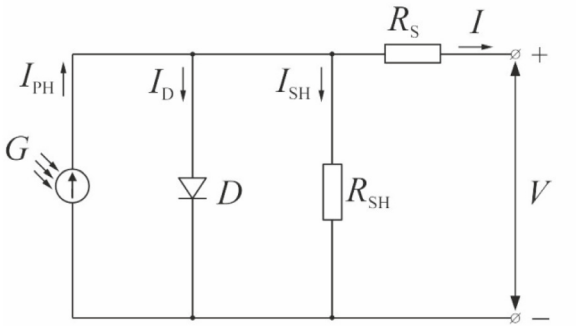

Fig. 2. The equivalent circuit of a solar cell.

3. Mathematical models of autonomous PV components

3.1. PV cell

To study the modes and characteristics of PV panel, in this work, a mathematical model is used that built on the basis of an equivalent electrical equivalent circuit of a solar cell with one diode (Ibrahim et al., 2019), as shown in Fig. 2.

The ideal model of a solar cell consists of a current source that creates an I_{PH} photocurrent, and an ideal diode (D), the current I_D through which is determined by the Shockley equation and depends on the absolute temperature (T) and voltage (V) at the output of the PV panel.

Using generally accepted assumptions, I_{PH} and the reverse current of the diode I_0 can be determined from the following expressions:

$$I_{PH} = [I_{SC\_STC} + k_I \cdot (T - T_{STC})] \cdot G, \tag{1}$$

where I_{SC_STC} is the short circuit current of the photovoltaic converter under standard conditions; k_I is the temperature coefficient of short circuit current; T_{STC} is the cell temperature under standard conditions; G is the value of solar irradiance, W/m^2.

$$I_0 = \left[\frac{I_{SC\_STC}}{\exp\left(\frac{q \cdot V_{OC\_STC}}{A \cdot k \cdot T_{STC}}\right) - 1}\right] \cdot \left(\frac{T}{T_{STC}}\right)^3 \cdot \exp\left[\frac{q \cdot E_G}{k \cdot A}\left(\frac{1}{T_{STC}} - \frac{1}{T}\right)\right], \tag{2}$$

where $q = 1{,}602 \cdot 10^{-19}$ C; $k = 1.38 \cdot 10^{-23}$ J/°K — Boltzmann constant; A is the diode ideality coefficient (takes values from 1 to 5); E_G-semiconductor band gap (determined by the type of SC used).

For a photovoltaic module, consisting of N_S series and N_P, parallel connected panels, the equation of the current–voltage characteristic has the following form:

$$I = N_P \cdot I_{PH} - N_P \cdot I_0 \cdot \left[\exp\left(\frac{q(V + I \cdot R_S)}{N_S \cdot A \cdot k \cdot T}\right) - 1\right] - \frac{V + I \cdot R_S}{R_{SH}}, \tag{3}$$

where I, V are the current and voltage at the terminals of the PV module; R_S and R_{SH} are equivalent series and shunt resistances of the photovoltaic module, respectively.

Eq. (3) contains five unknown parameters (I_{PH}, I_0, A, R_S, R_{SH}), which are dependent on the surface temperature of the PV string and the intensity of solar irradiance. The technical specification provides important points of the energy characteristics of the PV panel: I_{SC} short circuit current, the analytical expression for which can be obtained from (3), substituting $V = 0$ into it; open circuit voltage V_{OC} corresponding to the voltage value at the PV panel terminals with an open external circuit ($I = 0$). The parameters

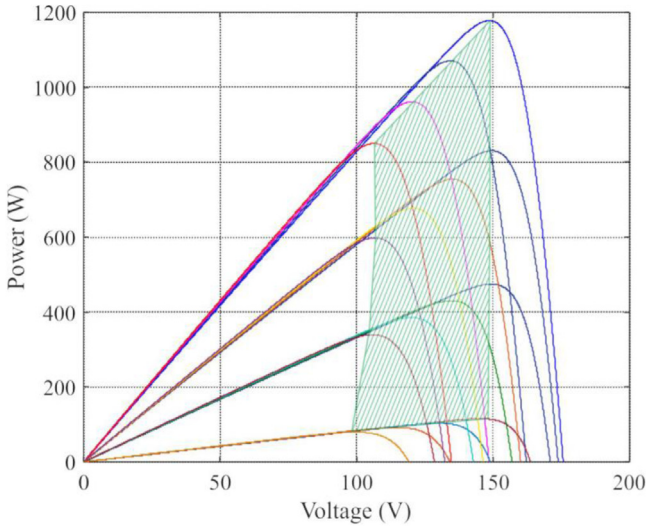

Fig. 3. Volt–watt characteristics of PV panel.

of the operating mode for the load corresponding to the point of maximum power at which $I = I_{MPP}$, $V = V_{MPP}$ are also given.

Using the data of the technical specification of PV panel, it is possible to obtain a numerical solution of Eq. (3) and construct a dynamic mathematical model of PV. For simulation of PV modes, the PV Array standard block from the MATLAB/Simulink library, built on the basis of Eqs. (1)–(3), was used as a PV model.

To select the parameters of the DC-converter, it is necessary to set the operating range of its input voltage, which is determined by the values of the irradiance G and temperature T_{FM} of the PV modules. Fig. 3 shows the "family" of volt–watt characteristics of a solar battery, consisting of three Kyocera Solar KD320GX-LPB FM modules in series (the Kyocera polycrystalline module combines the highest energy efficiency with an enviable rated power and stylish design, so it is an undoubted leader in sales for several years), built on the basis of simulation results. The characteristics are built at discrete set values of G = 100, 400, 700, 1000 W/m^2 and $T_{FM} = -25$, 0, 25, 50 °C, which corresponds to the ranges of the external climatic conditions under which electric power generation of photovoltaic systems is possible. The shaded area, in Fig. 3, defines the working range of the input voltage of the DC converter and its power.

The task of determining the operating range of input voltages and the nominal power of the DC–DC converter can be significantly simplified by solving it analytically using the technical specification of the PV panel, and also assuming that when the external climatic conditions change, the voltage in MPP changes in proportion to the open-circuit voltage, and the current in MPP changes in proportion to the photocurrent. Then, to determine V_{MPP} and I_{MPP} for arbitrary values of G and T_{FM}, the following equations can be used (Ibrahim et al., 2019; Obukhov et al., 2020):

$$I_{MPP} = [I_{MPP\_STC} + k_I \cdot (T_{FM} - T_{STC})] \cdot N_{FMp} \cdot \frac{G}{G_{STC}}, \tag{4}$$

$$V_{MPP} = [V_{MPP\_STC} + k_V \cdot (T_{FM} - T_{STC})] \cdot N_{FMs} - [(I_{MPP\_STC} - I_{MPP}) \cdot R_S] \cdot \frac{N_{FMs}}{N_{FMp}}, \tag{5}$$

where V_{MPP_STC} and I_{MPP_STC} are voltage and current in MPP under standard testing conditions (G_{STC} = 1000 W/m^2, T_{STC} = 25 °C); N_{FMs} and N_{FMp} are the numbers of series-connected and parallel-connected panels in the PV string, respectively; R_S is the series resistance of the PV module.

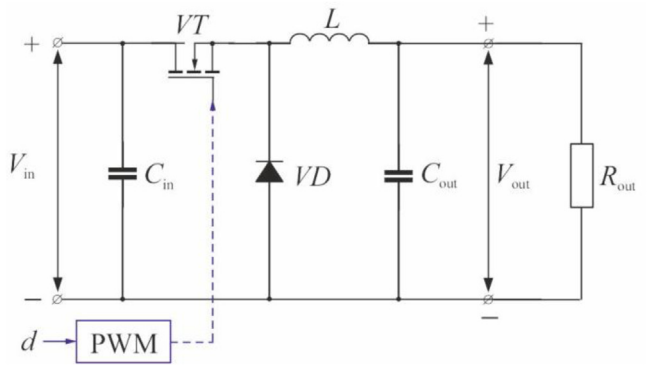

Fig. 4. Schematic diagram of DC–DC buck converter.

The value of R_S is determined by the expression (Ibrahim et al., 2019):

$$R_S = \frac{\frac{N_S \cdot A \cdot k \cdot T_{STC}}{q} \cdot \ln\left(1 - \frac{I_{MPP\_STC}}{I_{SC\_STC}}\right) + V_{OC\_STC} - V_{MPP\_STC}}{I_{MPP\_STC}}, \quad (6)$$

where N_S is the number of series solar cells in the module.

The above simplified approach for determining the parameters of the MPP PV mode with obvious ease of use provides a sufficiently high accuracy. A comparison of the results of calculating the voltage and current values in the MPP PV panel obtained by Eqs. (4)–(6), with the simulation results of the characteristics of the PV obtained by the numerical solution of Eqs. (1)–(3), shows that the maximum error in the determination of V_{MPP} and I_{MPP} in the entire practical range of changes in G and T_{FM} is not more than 4%.

3.2. DC–DC buck converter

The circuit diagram of the buck converter is shown in Fig. 4.

The main elements of the converter are input capacitive filter C_{in}, transistor switch VT, output LC-type smoothing filter on the L and C_{out} elements, and a discharge diode VD. The power supply of the converter is the PV panel, the output terminals are connected to the resistance Rout, which simulates the output load of the PV. The transistor switch control signal is supplied from a pulse width modulation (PWM) generator and is generated based on the values of the duty cycle d calculated by the MPPT controller.

In most practical cases, the converter is designed to operate in continuous current mode (CCM), which ensures its better controllability and minimization of energy loss. The timing diagrams of an ideal converter for the continuous current mode of the inductor are shown in Fig. 5.

If the ripples of the output voltage are neglect, from Fig. 5, the ripple current of the inductor can be expressed:

$$\Delta i_L = I_{L(\max)} - I_{L(\min)} = \frac{V_{in} - V_{out}}{L} \cdot t_{on} = \frac{V_{out}}{L \cdot f} \cdot \left(1 - \frac{V_{out}}{V_{in}}\right) = \frac{V_{out} \cdot (1-d)}{L \cdot f}, \quad (7)$$

where t_{on} is the time interval of the conducting state of the key; t_{off} – pause time interval; $T_0 = 1/f$ is the period of the pulse-width modulated pulses; f is the switching frequency; $d = t_{on}/T_o = V_{out}/V_{in}$–duty cycle or relative pulse duration.

To preserve the CCM up to the minimum load current, the following condition must be fulfilled: $\Delta i_L = 2 \cdot I_{out}$ (min). Fulfillment of this condition will provide a CCM, however, a large ripple negatively affects the saturation of the inductor core and the quality of the output voltage of the converter. Therefore, in practice, the value of current ripple is limited by the choice of the corresponding ripple coefficient $k_{\Delta i} = \Delta i_L/I_{out}$, the value of which is usually taken within 20%–50%. Then, taking into account (7), we obtain the condition for choosing L:

$$L \geq \frac{V_{out}}{k_{\Delta i} \cdot f \cdot I_{out(\min)}} \cdot \left(1 - \frac{V_{out}}{V_{in}}\right) = \frac{R_{out(\max)} \cdot (1-d)}{k_{\Delta i} \cdot f}. \quad (8)$$

The value of the ripple of the output voltage of the converter can be determined by assuming that the AC component of the current is closed only through the filter capacitor C_{out} (Obukhov et al., 2016b). Given that the maximum ripple current corresponds to the mode $d = 0.5$, from Fig. 5, one can express the change in charge on the output capacitor:

$$\Delta Q = \frac{1}{2} \cdot \left(\frac{T_0}{2}\right) \cdot \left(\frac{\Delta i_L}{2}\right) = \frac{\Delta i_L}{8 \cdot f}. \quad (9)$$

Taking into account that the voltage ripple and the change in the charge of the capacitance are related by the relation $\Delta V = \Delta Q/C$ from (7) and (9), the condition for choosing a filter capacitor can be expressed as:

$$C_{out} \geq \frac{V_{out} \cdot (1-d)}{8 \cdot L \cdot f^2 \cdot \Delta V_{out}} = \frac{(1-d)}{8 \cdot L \cdot f^2 \cdot k_{\Delta Vout}}, \quad (10)$$

where $k_{\Delta Vout} = \Delta V_{out}/V_{out}$ is the permissible ripple coefficient of the output voltage, this value can be determined by the requirements of the load (usually 1%–5%).

An obligatory element of the converter is the input capacitor C_{in}, which provides smoothing of the voltage ripples of the PV panel due to the nonlinearity of its characteristics. The capacitor C_{in} is selected from the condition that the ripple of the input voltage of the converter is limited to no more than $k_{\Delta Vin} = 1\%$, which will ensure the most efficient use of the energy generated by the PV panel (Korshunov, 2005). Taking into account (7), (9), (10), the condition for choosing the input capacitor of a step-down voltage converter can be represented in the form of the expression:

$$C_{in} \geq \frac{V_{in} \cdot d \cdot (1-d)}{8 \cdot L \cdot f^2 \cdot \Delta V_{in}} = \frac{1}{32 \cdot k_{\Delta Vin} \cdot L \cdot f^2}. \quad (11)$$

The most important task of designing voltage converters is the calculation and analysis of their dynamic characteristics. PWM voltage converters belong to nonlinear discrete automatic control systems, to determine the dynamic characteristics of which are widely used analysis methods based on approximate averaged models of converting devices (Ayop and Tan, 2018). The transfer functions of the buck DC–DC converter according to the control action obtained from the linearized averaged model (Belov and Serebryannikov, 2008) will be written in the following form:

$$W_{\Delta d}^{\Delta V_{out}}(s) = \frac{V_{in}}{L \cdot C_{out}} \cdot \frac{1}{s^2 + \frac{s}{R_{out} \cdot C_{out}} + \frac{1}{L \cdot C_{out}}};$$

$$W_{\Delta d}^{\Delta I_{out}}(s) = \frac{V_{in}}{L} \cdot \frac{s + \frac{1}{R_{out} \cdot C_{out}}}{s^2 + \frac{s}{R_{out} \cdot C_{out}} + \frac{1}{L \cdot C_{out}}}. \quad (12)$$

Eqs. (12) describe the response of the output voltage and current of the converter to a change (deviation relative to the linearization point) of the duty ratio d. The obtained Eq. (12) allows us to analyze the frequency characteristics of the converter and synthesize a control system built on the basis of traditional analog controllers.

3.3. The output loads of the DC–DC converter

The nature of loads of the DC–DC voltage converter is determined by the power plant construction schema. For a PV constructed according to schema 1 (see Fig. 1), the operating

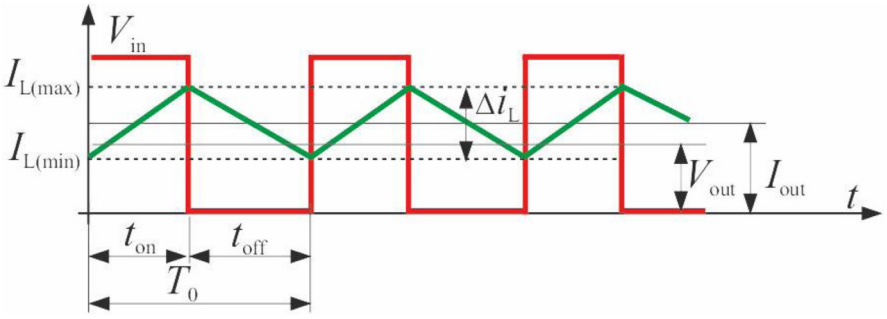

Fig. 5. Timing diagram of a buck converter for the continuous current mode of the inductor.

modes of the DC–DC converter can be considered equivalent to the operating conditions for the load with the same active resistance. In schema 2, the load of the converter is battery bank. In schema 3, DC–DC converter is loaded on a DC bus.

When constructing the simulation model of PV system, the load of the converter was modeled as a separate functional unit (Fig. 6), which makes it easy to change the configuration of the system under study.

The Battery standard block from the MATLAB/Simulink library is used as a dynamic model of the battery. The DC bus model is based on a C_{DC} capacitor and a DC voltage source with an internal resistance R_{DC}.

3.4. Maximum power controller

Depending on the hardware version, two main types of MPPT controllers are distinguished: analog and digital. In analog controllers, the control signal is formed in the form of a reference voltage, which is compared with the output voltage of the converter, then the mismatch signal is processed by a traditional control system based on a proportional-integral controller (Rashid, 2011). In digital controllers, the output signal is the duty cycle, d, which is fed directly to the converter transistor keys through the PWM generator. Due to the simplicity of implementation and high reliability, the MPP digital controllers are mainly used in modern PV systems (Shebani et al., 2017). When using digital controllers, the value of d changes discretely by the value of Δd after a certain sampling time t_s (sample time) (Loukriz et al., 2017). However, the numerical values directly affect the accuracy and speed of MPP tracking when the solar irradiance and temperature of the PV are changed. Accordingly, the main task of designing digital MPPT controllers is to determine the optimal values of Δd and t_s, which ensure maximum accuracy and speed of MPP tracking.

In this paper, a digital MPPT controller that implements the incremental conductance algorithm (IC) is considered. The principle of operation of the conductivity increment algorithm is based on the equality of the instantaneous conductivity of the PV panel and the derivative of the conductivity at the maximum power point (Obukhov et al., 2016b). Mathematical relations explaining the operation of the IC algorithm can be easily obtained by differentiating the power P of the solar battery with respect to voltage V, taking into account the fact that the derivative at the maximum power point vanishes:

$$dP/dV = d(V \cdot I)/dV = I + V(dI/dV) = 0. \tag{13}$$

Eq. (13) can be represented as:

$$dI/dV = -I/V. \tag{14}$$

Expression (14) implies two important relationships that allow to determine the position of the operating point of the PV on its voltage–power characteristics relative to the point of maximum power:

$$\left.\begin{aligned} \frac{dI}{dV} &> -\frac{I}{V}\left(\frac{dP}{dV} > 0\right) - \text{Left of MPP;} \\ \frac{dI}{dV} &< -\frac{I}{V}\left(\frac{dP}{dV} > 0\right) - \text{Right of MPP.} \end{aligned}\right\} \tag{15}$$

Taking into account relations (15), the operation of the IC algorithm can be represented in the form of a block diagram shown in Fig. 7. In the PV simulation model, the IC algorithm model is implemented as a function program in the m-file in MATLAB/Simulink.

The main task of designing digital MPPT controllers is to determine the clock frequency f_d of the change in the duty cycle of the DC–DC converter.

It is advisable to select the value of f_d from the condition of stable operation of the control system, which is ensured if the transient process in the converter, caused by a change in the control action or external conditions, ends in the time $t_s = 1/f_d$.

The time constant of the step-down DC–DC converter τ can be approximately found from the equation:

$$\tau = \frac{L}{R_{out}}. \tag{16}$$

According to that the duration of any transient process is up to 5 of τ, it is recommended to use the expression to determine the optimal value of t_s:

$$t_s \geq 5 \cdot \tau. \tag{17}$$

The choice of the value of t_s according to condition (17) will ensure maximum performance of the MPPT controller and at the same time stable operation in MPP.

For determining the parameters of the MPPT controller, the load nature of the DC–DC converter must be considered. For PV constructed according to schema 1, the value of the equivalent electrical load is uniquely determined by this expression:

$$R_{out} = R_{load}. \tag{18}$$

In PV, according to schema 2 and 3, the voltage at the converter output is stabilized. Neglecting the change in voltage on the battery bank clamps from the value of its charge and without taking into account the statism of the DC bus, the value of the equivalent resistance of the DC–DC converter can be determined through the output power. For an ideal converter with a stabilized output voltage, the equivalent output resistance is determined by the formulas:

$$R_{out(min)} = \frac{V_{out}^2}{P_{MPP(max)}}; \quad R_{out(max)} = \frac{V_{out}^2}{P_{MPP(min)}}, \tag{19}$$

where P_{MPP} (max), P_{MPP}(min) are the values of the maximum and minimum powers generated by the PV module.

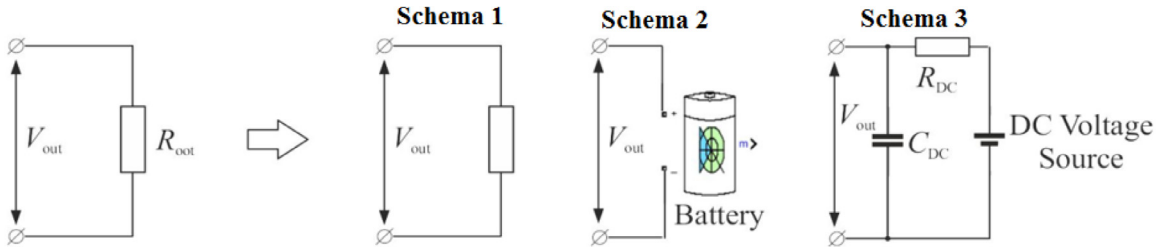

Fig. 6. The simulation model of the different loads of the DC–DC Converter of the photovoltaic station.

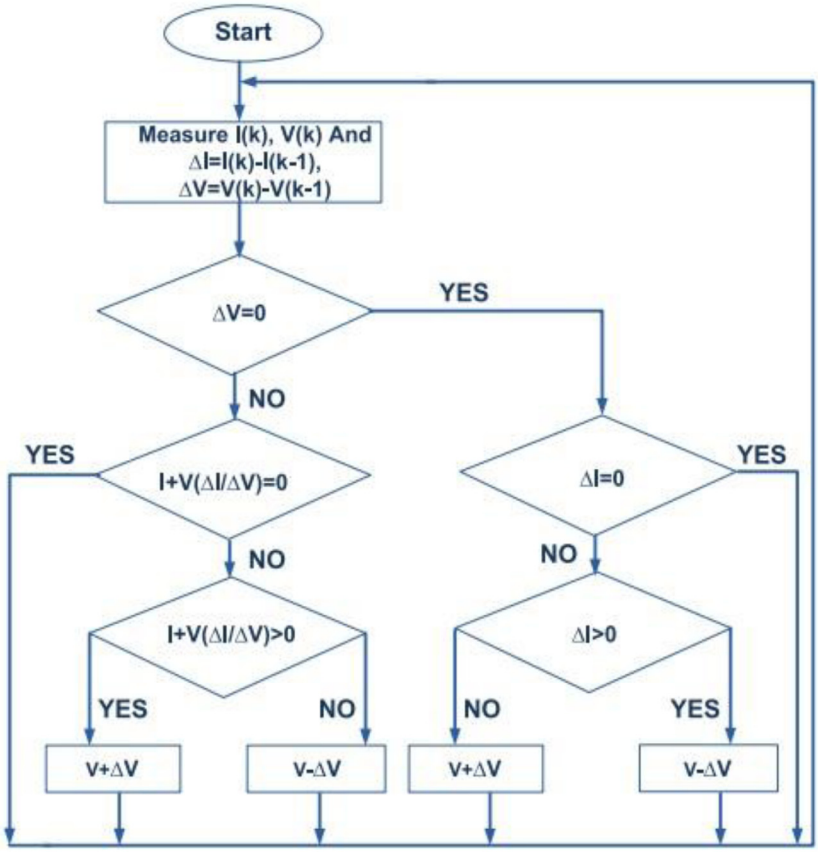

Fig. 7. Flowchart for the incremental conductance algorithm.

Since the converter time constant is inversely proportional to R_{out}, it is necessary to substitute the minimum value of the equivalent resistance determined by (19) into Eq. (16).

An important parameter of the digital MPPT controller is the value of the change in the operating cycle of the converter Δd during the sampling time ts. A large Δd value shortens the MPP search time, but this reduces the tracking accuracy and can also lead to an oscillatory mode near MPP. It can be approximately assumed that the magnitude of the step in changing the output power of the PV panel ΔP linearly depends on the value of Δd. With this assumption, to determine the optimal value of Δd, you can use the equation:

$$\Delta d = \frac{\varepsilon}{100} \cdot (d_{\max} - d_{\min}), \tag{20}$$

where ε is the permissible relative error (%); dmin, dmax are the minimum and maximum values of the duty cycle, respectively. The results of the studies showed that a good compromise between the speed and accuracy of tracking MPP provides the value $\varepsilon = 1\%$, which was used in the computational experiments.

4. Matching the PV and voltage converter parameters for achieving the MPP

Eqs. (1)–(3) determine the form of the current–voltage characteristics of the PV panel, which depend on the level of illumination G and the surface temperature T. Fig. 8 shows the I-V characteristics of the PV panel for different levels of solar irradiance and temperature.

On each of the I – V characteristics, there is a single point (in Fig. 8 designated as A and B), corresponding to certain values of the current I_{MPP} and voltage V_{MPP}, at which the PV panel will generate the maximum power P_{MPP}.

These voltage and current values determine the equivalent PV panel resistance at the maximum power point:

$$R_{MPP} = \frac{V_{MPP}}{I_{MPP}}. \tag{21}$$

The maximum power with PV panel is ensured when the equivalent output resistance of the PV module in MPP R_{MPP} and the equivalent input resistance of the converter R_{in} are equal. The

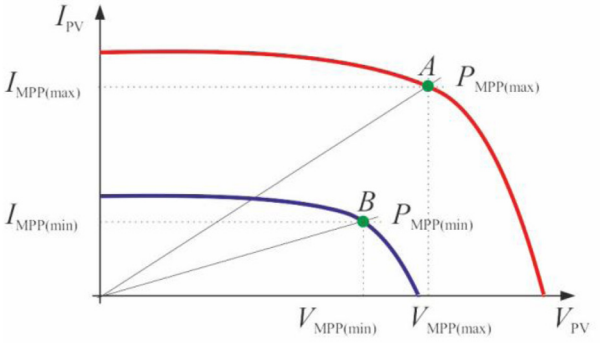

Fig. 8. Volt–current characteristic of PV panel under different solar irradiance and temperature conditions.

Table 1
Key points the solar panels of a photovoltaic station.

Solar irradiance (G)	Temperature (T)	Indicators	Mode
min	min	$R_{MPP(max)}$, $I_{MPP(min)}$	Maximum resistance
min	max	$P_{MPP(min)}$, $V_{MPP(min)}$	Minimum power
max	min	$P_{MPP(max)}$, $V_{MPP(max)}$	Maximum power
max	max	$R_{MPP(min)}$, $I_{MPP(max)}$	Minimum resistance

value of R_{in} depends on the converter topology, its load R_{out} and the duty cycle value d (duty cycle). When searching for MPP, controller changes the value of d so that the condition is satisfied: $R_{MPP} = R_{in}$. If we neglect the losses in the step-down DC-converter, an important practical relation is derived from the condition of equality of its input and output power:

$$\frac{V_{MPP}^2}{R_{MPP}} = \frac{V_{out}^2}{R_{out}} = \frac{(V_{MPP} \cdot d)^2}{R_{out}} \Rightarrow d = \sqrt{\frac{R_{out}}{R_{MPP}}}. \quad (22)$$

Since the value of d cannot be greater than 1, it follows from (22) that the output resistance of the buck converter must be less than the minimum equivalent resistance of the PV panel in MPP in order to ensure the PV module in MPP in all possible operating modes:

$$R_{out} < R_{MPP(min)}. \quad (23)$$

When designing the converter for PV system; built according to schemes 2 and 3, this condition is transformed into the choice of the rational value of the nominal output voltage of the converter according to the condition, where:

$$V_{out} < V_{MPP(min)}. \quad (24)$$

A characteristic feature of PV panel is the direct dependence of I_{MPP} and the inverse dependence of V_{MPP} on the surface temperature of the module, with the temperature coefficient of voltage k_V in absolute value far exceeding the temperature coefficient of current k_I. Analysis of the V–P characteristics PV panel (see Fig. 3) shows that, for designing a converter, it is necessary to determine the current and voltage values in MPP for four nodes at various combinations of G and T. Characteristics of the PV panel nodes and their corresponding indicators modes are given in Table 1.

The minimum and maximum values of G and T are determined in accordance with the location and operating conditions of the PV panel. In the present studies, the ranges of the radiation and temperature changes, characteristic for the operating conditions of photovoltaic power plants in the northern latitudes are determined as follows: $G_{min} = 100$ W/m^2, $G_{max} = 1000$ W/m^2, $T_{min} = -25$ °C, $T_{max} = +50$ °C.

The values of currents, voltages and power at the nodal points of the PV panel are easily determined by Eqs. (4)–(6). The values of equivalent resistances are calculated by Eq. (21). To determine the limiting values of the duty cycle of the buck converter, Eq. (22) is used.

Table 2
Electrical parameters of the Kyocera Solar KD320GX-LPB PV module.

Parameter	Value
Open-circuit voltage, V_{OC}, V	49,5
Short circuit current, I_{SC}, A	8,6
Voltage at P_{MPP} , V_{MPP} V	40,1
Current at P_{MPP}, I_{MPP} A	7,99
Maximum power, P_{MPP}W	320,4
Open circuit voltage coefficient V_{OC}, k_V V/°C	−0,1832
Short circuit current coefficient I_{SC}, k_I A/°C	0,00328
Number of cells connected in series, N_S	80

5. Method of calculation and selection of parameters of basic elements of the PV system

Based on the analysis of the energy characteristics of the main elements of the PV system, a methodology has been developed for calculating and selecting their optimal parameters, presented in the form of a flowchart shown in Fig. 9.

When using the proposed method it is necessary to consider features of modes of DC–DC-converter for loads of different nature. This feature can be noted when operating on a load in the form of a constant resistance (Schema 1), an increase in d values leads to an increase in the output power of the converter, while in power systems with a stabilized output voltage of the converter (Schema 2, 3), an increase in d causes a decrease in the output power. Accordingly, when calculating the parameters of the DC–DC converter for circuit 1 in Eqs. (8) and (10), the minimum duty cycle dmin must be used, for circuits 2 and 3, d_{max} must be used in Eq. (8), and in Eq. (10) — d_{min}.

6. Results and discussion

To test the proposed methodology, we considered a practical example of calculating and selecting the parameters of a DC–DC converter and a digital MPPT controller of an autonomous PV system built on the basis of an PV consisting of three series-connected Kyocera Solar KD320GX-LPB, the main technical characteristics are given in Table 2.

For completeness of the analysis, three possible options for constructing autonomous PV were considered; schemes 1–3. For each circuit, simulation models of PV station based on the mathematical models of the components presented above were developed and implemented in the MATLAB/Simulink software environment. To increase the reliability of the results and evaluate the efficiency of energy conversion in the FES simulation model, the non-ideality of the converter elements – the active resistance of the inductor and the equivalent internal resistance of the capacitors, as well as the static characteristics of the transistor and diode – voltage drop and resistance in the conducting state are taken into account.

The parameters of the DC–DC converter and MPPT controller were calculated and selected by the proposed method in accordance with the block diagram shown in Fig. 9. In the FES simulation model for circuit 2, a lead–acid battery with a nominal capacity of 200 A h is adopted as an energy storage device, the DC bus model in circuit 3 was built on the basis of a 300 μF capacitor and an active resistance of 0.01 Ω. The frequency of the PWM generator (f) in all computational experiments was taken equal to 25 kHz.

The parameters of the DC–DC converter and MPPT controller, selected as a result of calculation by the proposed method, are given in Table 3.

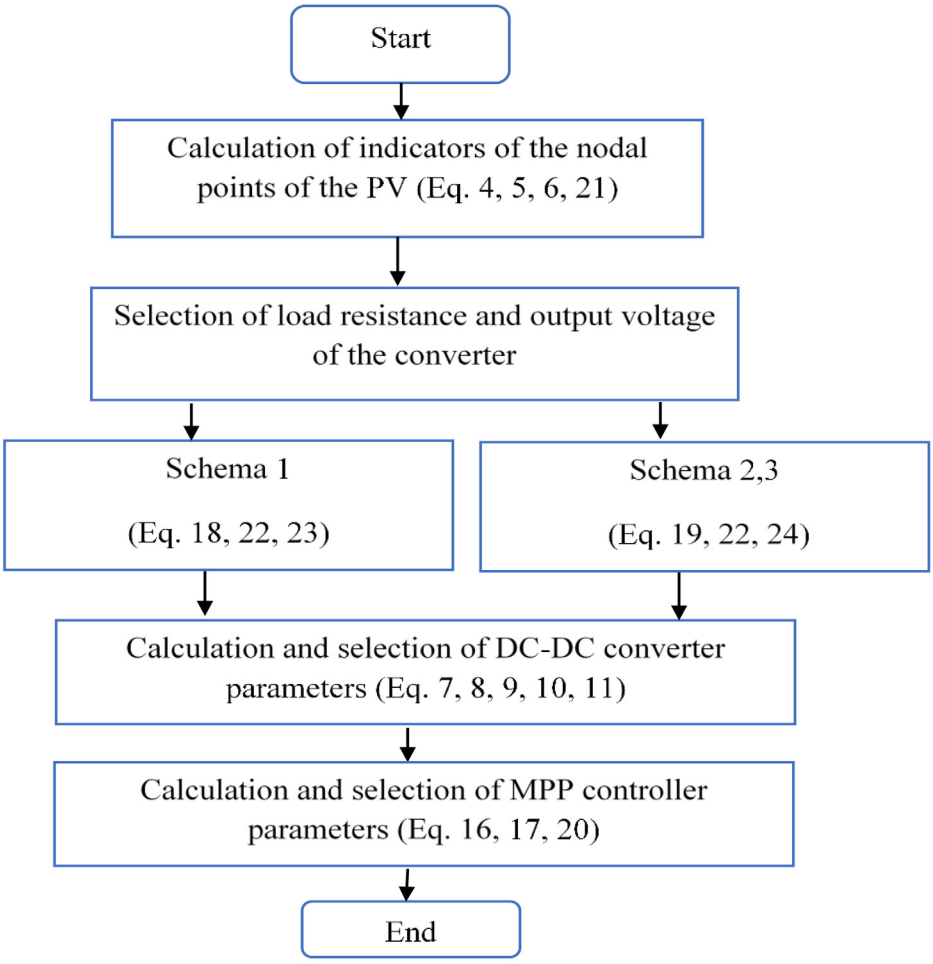

Fig. 9. Flowchart for calculating and selecting optimal parameters of the main elements of an autonomous photovoltaic station.

Table 3
Results of calculation and selection of parameters of the main components of an Autonomous photovoltaic station.

Parameter	Value	
	Schema 1	Schema 2, 3
R_s, Ω	0,487	0,487
R_{out}, Ω	10	–
V_{out}, V	–	48
d_{min}	0,24	0,33
d_{max}	0,87	0,50
L, μH	800	1500
C_{out}, μF	20	10
C_{in}, μF	20	10
t_s, s	0,0004	0,004
Δd	0,005	0,0015

The calculation results show that the inertia of a DC–DC converter, designed to operate as a part of autonomous photovoltaics, which is constructed according to schemes 2 and 3 is an order of magnitude higher than that of a similar converter operating on an active load. In addition, from the Table 3 it is obvious that for a DC–DC converter with a stabilized output voltage, the working range of the duty cycle changes significantly, which determines the high rigidity of its adjustment characteristics, and accordingly, increases the requirements for accuracy and quality of regulation of the control system.

Fig. 10 shows the results of modeling the operating modes of the FES with a sudden change in the lighting conditions of the SB for circuits 1 and 2 (the results for circuit 3 are not given, since they are almost identical to circuit 2). When carrying out this computational experiment, the lighting conditions of the SB change after 0.05 s of model time and correspond to the following successive values of solar radiation: G = 800; 400; 200; 600; 1000 W/m^2. The surface temperature of the PM is assumed unchanged −25 °C.

During the computational experiments, the values of the duty cycle d (duty cycle), output power (PV Power), voltage (PV Voltage) and current (PV Current) of solar batteries, as well as the parameters of the electric energy consumed by the load were recorded.

The simulation results presented in Fig. 10 prove that the DC–DC converter and the MPPT controller with the selected parameter values provide reliable and efficient MPP tracking in all 5 test variants of the illumination change. The tracking accuracy of the maximum power point in scheme 1 is at least 99.6%, in scheme 2 it is at least 98.2%, and the efficiency of the DC–DC converter in all the considered modes did not fall below 93.2%. The operating ranges for changing the energy characteristics of the main elements of the PV system (current, voltage, power) correspond to the calculated values obtained during their design.

An interesting feature of the dynamic modes of an autonomous PV is as follows: despite the fact that circuit 2 has a much greater inertia than circuit 1, the transients in it, caused by a sudden change in the illumination of the PV panel, end much faster. This is explained by the fact that a change in the value of solar irradiance insignificantly affects the voltage in the MPP PV (see Fig. 3), and in circuits with a stabilized output voltage of the converter, the value of the duty cycle d remains practically unchanged,

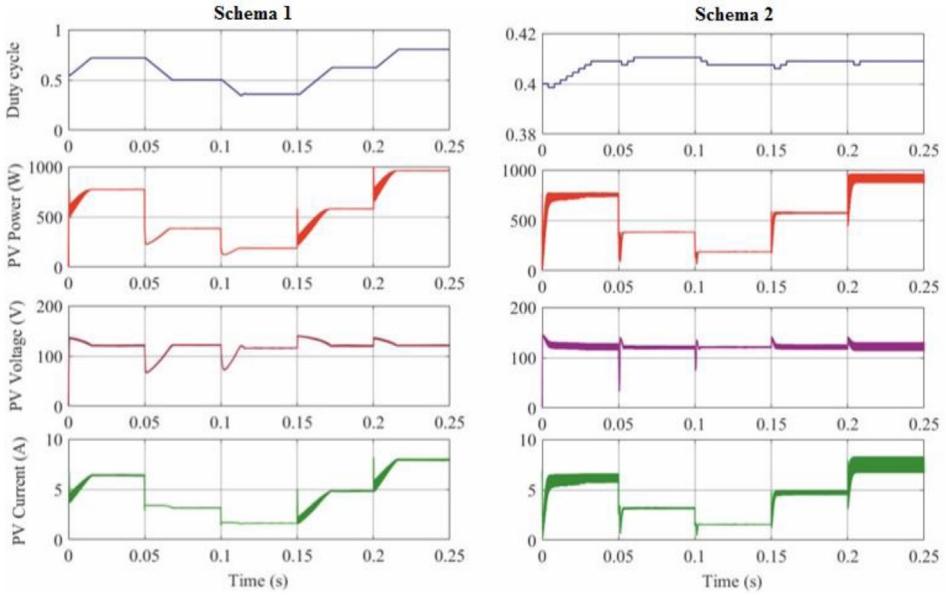

Fig. 10. Results of simulation of photovoltaic station modes under changing lighting conditions by solar panels.

which ensures a quick end of the transient process. The value of d depends much more strongly on the surface temperature of the photovoltaic modules, which cannot change instantly or with a high gradient commensurate with the time constant of the DC–DC converter, and this dependence is not critical. When a DC–DC converter operates on an active resistance, the value of its output voltage changes in proportion to the supply voltage, which requires a change in the value of *d* within a fairly wide range. With correctly selected parameters of the converter and MPPT controller, the MPP tracking time does not exceed 0.03 s, which is obvious from Fig. 10.

7. Conclusion

The article presents an original methodology for calculating and choosing optimal parameters for the main elements of an autonomous PV systems; a buck DC–DC converter and a MPPT controller. The parameters of the converter are selected on the basis of calculation and analysis of the possible range of voltage changes at the point of maximum power under various lighting conditions and temperatures. The parameters of the digital MPPT controller are selected based on the calculated value of the converter time constant and the nature of its electrical load. The paper considers three main options for constructing autonomous PV, for each of which design features are established. The proposed method has been tested on a specific example, its adequacy is confirmed by the results of the simulation of dynamic modes of an autonomous PV for all three considered topologies.

CRediT authorship contribution statement

H.I. Abdul-Ghaffar: Funding acquisition. **Ahmed A. Zaki Diab:** Investigation.

Declaration of competing interest

The authors declare that they have no known competing financial interests or personal relationships that could have appeared to influence the work reported in this paper.

Acknowledgment

This research was supported by Tomsk polytechnic university development program.

References

Amir, A., Amir, A., Che, H.S., et al., 2019. Comparative analysis of high voltage gain DC-dc converter topologies for photovoltaic systems. Renew. Energy 136, 1147–1163.

Anon, 0000. Decree of the Government of the Russian Federation of May 28, 2013 (449) On the mechanism for stimulating the use of renewable energy sources in the wholesale market of electric energy and power, Published on the official Internet portal of legal information http://www.pravo.gov.ru.

Ashurov, Kh.B., Abdurakhmanov, B.M., Iskandarov, Sh.Ch., et al., 2019. Solving the problem of energy storage for solar photovoltaic plants (review). Appl. Sol. Energy 55 (2), 119–125.

Avezova, N.R., Vokhidov, A.U., Farmonov, A.A., Dalmuradova, N.N., 2019. Renewable energy: challenges and solutions. Appl. Sol. Energy 55 (2), 149–152.

Ayop, R., Tan, C. Wei, 2018. Design of boost converter based on maximum power point resistance for photovoltaic applications. Sol. Energy 160, 322–335.

Belov, G., Serebryannikov, A., 2008. Structural dynamic models and the frequency method for the synthesis of dual-circuit control systems for pulse converters. Power Electron. 3, 98–106.

Chauhan, A., Saini, R.P.., 2014. A review on integrated renewable energy system based power generation for stand-alone applications: Configurations. Storage Options Sizing Methodol. Control 38, 99–120.

Chetti, P., 1990. Designing Key Power Supplies. M.: Energoatomizdat, p. 238.

Ibrahim, A., Aboelsaud, R., Obukhov, S., 2019. Improved particle swarm optimization for global maximum power point tracking of partially shaded PV array. Electr. Eng. 101 (2), 443–455. http://dx.doi.org/10.1007/s00202-019-00794.

Jäger-Waldau, A., 2018. European Commission, and Joint Research Centre. {PV} status report 2018 study.

Khatib, T., Ibrahim, I.A., Mohamed, A., 2016. A review on sizing methodologies of photovoltaic array and storage battery in a standalone photovoltaic system. Energy Convers. Manage. 120, 430–448.

Korshunov, A., 2005. Dynamic calculation of a stabilized step-down DC-DC voltage converter. Power Electron. 3, 88–91.

Loukriz, A., Haddadi, M., Messalti, S., 2017. Simulation and experimental design of a new advanced variable step size incremental conductance MPPT algorithm for PV systems. ISA Trans. 30–38.

Mack, R., 2008. Switching Power Supplies. In: Theoretical Design Basics and Practical Application Guidelines, M.: Dodeka-XXI Publishing House, p. 272.

Nayak, B., Mohapatra, A., Mohanty, K.B., 2017. Selection criteria of dc-dc converter and control variable for MPPT of PV system utilized in heating and cooking applications. Cogent Eng. 4, 1–16.

Obukhov, S., Ibrahim, A., Diab, A.A.Z., Al-Sumaiti, A.S., Aboelsaud, R., 2020. Optimal performance of dynamic particle swarm optimization based maximum power trackers for stand-alone PV system under partial shading conditions. IEEE Access 20, 1–28.

Obukhov, S., Plotnikov, I., Kryuchkova, M., 2016a. Simulation of electrical characteristics of a solar panel. IOP Conf. Ser. Mater. Sci. Eng. 132, 012017.

Obukhov, S.G., Plotnikov, I.A., Sheryazov, S.K., 2016b. Methods of effective use of solar power system. In: 2016 2nd International Conference on Industrial Engineering, Applications and Manufacturing (ICIEAM). pp. 1–6.

Rashid, M.H., 2011. Power Electronics Handbook: Devices, Circuits and Applications, third ed. Butterworth-Heinemann, Oxford, p. 1409.

Renewable energy policy network for the 21st century (REN21), 2018. Renewables 2018 Global Status Report. Paris Renew. energy policy Netw. 21st Century.

Rezk, H., Fathy, A., Abdelaziz A.Y, 2017. A comparison of different global MPPT techniques based on meta-heuristic algorithms for photovoltaic system subjected to partial shading conditions. Renew. Sustain. Energy Rev. 74, 377–386.

Shebani, M.M., Iqbal, T., Quaicoe J.E, 2017. Comparing bisection numerical algorithm with fractional short circuit current and open circuit voltage methods for MPPT photovoltaic systems. In: Electrical Power and Energy Conference (EPEC). IEEE, pp. 1–5.